Inorganica Chimica Acta 372 (2011) 347–352

Contents lists available at ScienceDirect

Inorganica Chimica Acta

journal homepage: www.elsevier.com/locate/ica

Copper phosphates and phosphinates with pyridine/pyrazole alcohol co-ligands: Synthesis and structure

Ramasamy Pothiraja [a], Malaichamy Sathiyendiran [a], Alexander Steiner [b], Ramaswamy Murugavel [a,*]

[a] *Department of Chemistry, Indian Institute of Technology – Bombay, Powai, Mumbai 400 076, India*
[b] *Department of Chemistry, University of Liverpool, Crown Street, Liverpool L69 7ZD, UK*

A R T I C L E I N F O

Article history:
Available online 3 April 2011

Dedicated to S.S. Krishnamurthy.

Keywords:
Copper phosphate
Copper phosphinate
Synthesis
Spectroscopy
X-ray structures

A B S T R A C T

Copper phosphates, [Cu(dtbp)$_2$(pzet)$_2$]·H_2O (**1**) and [Cu(dtbp)$_2$(pyme)$_2$] (**2**), as well as copper phosphinate, [Cu(dppi)$_2$(pyet)$_2$] (**3**) have been synthesized by the reaction of copper acetate with di-*tert*-butyl phosphate (dtbp) or diphenyl phosphinate (dppi) in the presence of pyridine base having hydroxyl group, namely, 3,5-dimethylpyrazole-2-ethanol (pzet) or 2-(hydroxymethyl)pyridine (pyme) or 2-(2-hydroxyethyl)pyridine (pyet). Single crystal X-ray diffraction studies reveal that copper ion in all the three complexes is bonded to two phosphoryl ions (P(O)O$^-$) and two pyridine co-ligands. The crystal structure of **1** reveals that the hydroxyl group of the CH_2CH_2OH moiety of pzet ligand exhibits a positional disorder between the non-bonding position and the bonding position with respect to the central copper ion along the Jahn–Teller axis. Hence, the structure of **1** can be considered to exhibit both 'square-planar' and 'octahedral' coordination geometries simultaneously for the copper ion in the same complex. A similar situation for the –OH groups has not been observed in the complexes **2** and **3** and hence the coordination geometry around the copper ion is axially elongated octahedron.

1. Introduction

Complexation to copper enhances the biological activity of a wide variety of organic ligands [1–3]. For example, the copper complex of 3,5-dimethylpyrazole has higher antimicrobial activity (testing on *Staphylococcus aureus*, *Escherichia coli* and *Candida albicans*) than 3,5-dimethylpyrazole [4,5] and the copper complex of 2-acetyloxybenzoic acid (copper(II) aspirinate) is a more effective anti-inflammatory agent than aspirine itself [3,6,7]. Hence it is very important to study the interaction of copper(II) ion with various ligands, which are actively involved in the biological metabolism. Since phosphorus based ligands are playing an important role in many biological reactions, the study of interaction of phosphorus containing ligands with copper(II) is very important. Copper phosphate or phophonate or phosphinates based research is mostly focused on clusters or complexes having more than one copper ions in the view of interesting magnetic interactions and structural nature [8–15]. The structure and interaction of phosphorus based ligands with copper ions in monomeric complexes are relatively less investigated [16].

We have been studying various metal phosphates, phosphinates and phosphonates for purposes such as realizing framework models, precursors for ceramic materials, and models for hydrolase reactions, etc. [8–13,15–22]. As a part of our ongoing research, we have used di-*tert*-butyl phosphate and diphenyl phosphinic acid as phosphorus containing ligands along with the co-ligands, 3,5-dimethylpyrazole-2-ethanol (pzet), 2-(hydroxymethyl)pyridine (pyme) and 2-(2-hydroxyethyl)pyridine (pyet), and synthesized copper phosphate and phosphinate complexes, [Cu(dtbp)$_2$(pzet)$_2$]·H_2O (**1**), [Cu(dtbp)$_2$(pyme)$_2$] (**2**) and [Cu(dppi)$_2$(pyet)$_2$] (**3**). We have investigated herein the interaction of these phosphorus containing ligands with copper ion, in the presence of hydroxyl group containing Lewis bases with the aid of single crystal X-ray diffraction studies. One of the interesting aspects of these co-ligands is that these Lewis bases possess additional hydroxyl group for coordination to metal either through OH or O- depending on the pH of the solution [23,24].

2. Experimental

2.1. General

All the starting materials and the products were found to be stable toward moisture and air, and hence no specific precaution was taken to rigorously exclude air during the preparation or handling of the compounds. Elemental analyses were performed on a Carlo Erba (Italy) Model 1106 Elemental Analyzer. Infrared spectra were recorded on a Perkin-Elmer Spectrum One spectrometer as KBr diluted discs. UV–Vis spectra were obtained on a Shimadzu UV-260

---

* Corresponding author. Tel.: +91 22 25767163; fax: +91 22 25767152.
E-mail address: rmv@chem.iitb.ac.in (R. Murugavel).

0020-1693/$ - see front matter © 2011 Elsevier B.V. All rights reserved.
doi:10.1016/j.ica.2011.03.063

spectrophotometer. Magnetic susceptibility was measured on a PAR vibrating sample magnetometer. Commercial grade solvents were purified by employing conventional procedures and were distilled prior to their use [25]. Commercially available starting materials such as $Cu(OAc)_2 \cdot H_2O$ (Fluka), pyridine (S.d.Fine-Chem.), PCl_3 (S.d.Fine-Chem.), Bu^{t}OH (S.d.Fine-Chem.), conc. HCl (Merck), $AlCl_3$ (S.d.Fine-Chem.), diphenylphosphinic acid (Lancaster), 2-(hydroxymethyl) pyridine (Aldrich) and 2-(2-hydroxyethyl) pyridine (Aldrich) were used as received. 3,5-Dimethylpyrazole-2-ethanol was prepared by condensation of acetylacetone with H_2NNHCH_2-CH_2OH. Di-*tert*-butylphosphate (dtbp-H) has been synthesized and purified as described previously [26].

2.2. Synthesis of **1**

A methanol solution of dtbp-H (210 mg, 1 mmol in 25 mL) was added to a solution of copper acetate (100 mg, 0.5 mmol in 5 mL methanol). To the resulting solution, solid pzet (140 mg, 1 mmol) was added under constant stirring. The stirring was continued for 15 min, solvent was removed under vacuum, and resulting blue solid was dissolved in THF. Blue crystals of **1** were obtained from this solution after 72 h. The crystals were re-dissolved in diethyl ether and kept at −15 °C to obtain dark blue single crystals of X-ray diffraction quality. Yield: 279 mg (72%). *Anal.* Calc. for $C_{30}H_{62}CuN_4O_{11}P_2$ (M_r = 780.3): C, 46.2; H, 8.0; N, 7.2. Found: C, 45.9; H, 7.9; N, 6.9%. IR (KBr, cm^{-1}): 3435 (br), 2975 (vs), 2928 (s), 1636 (w), 1557 (s), 1479 (s), 1444 (s), 1394 (s), 1368 (s), 1318 (s), 1249 (s), 1180 (s), 1063 (vs), 985 (vs), 913 (s), 875 (s), 829 (s), 818 (s), 780 (s), 706 (s), 604 (s), 516 (s). UV–Vis (CH_3OH, nm): 304, 770.

2.3. Synthesis of **2**

$Cu(OAc)_2 \cdot H_2O$ (199 mg, 1 mmol) was dissolved in methanol (40 mL) and dtbp-H (420 mg, 2 mmol) was added. To this, 2-(hydroxymethyl) pyridine (0.2 mL, ~2 mmol, in acetonitrile 30 mL) was added. The resulting solution was filtered and the filtrate was kept at room temperature for crystallization. X-ray diffraction quality single crystals were obtained after 1 week. Yield: 0.51 g (73%). Mp 139 °C. *Anal.* Calc. for $C_{28}H_{50}CuN_2O_{10}P_2$ (M_r = 700.2): C, 48.0; H, 7.2; N, 4.0. Found: C, 47.8; H, 7.4; N, 4.2%. IR (KBr, cm^{-1}): 2979 (m), 2934 (m), 1365 (m), 1250 (s), 1180 (s), 1056 (vs), 978 (s), 825 (m), 716 (m). UV–Vis (CH_3OH, nm): 288, 742. TGA: temperature range, °C (% weight loss): 103–185 (47.6); 186–325 (15.5); 326–792 (5.3). DSC (°C): 144 (endo); 160 (endo); 211 (endo). μ_{found} = 1.73 BM, g = 2.09 (300 K), 2.08 (77 K), 2.03 (77 K, CH_2Cl_2).

2.4. Synthesis of **3**

To a solution of $Cu(OAc)_2 \cdot H_2O$ (100 mg, 0.5 mmol in 20 mL methanol), dppi-H (218 mg, 1 mmol) and 2-(2-hydroxyethyl) pyridine (0.25 mL, ~2 mmol) were added. The resulting solution was stirred for 2 min and the solvent was removed under vacuum. The resulting waxy solid was dissolved in Et_2O/MeOH (1:1) and kept at room temperature for crystallization. X-ray diffraction quality crystals were obtained after 2 weeks. Yield: 0.6 g (81%). Mp 115 °C. *Anal.* Calc. for $C_{38}H_{38}CuN_2O_6P_2$ (M_r = 744.2): C, 61.33; H, 5.15; N, 3.76. Found: C, 59.2; H, 5.5; N, 4.3%. IR (KBr, cm^{-1}): 3120 (br), 3070 (m), 2946 (w), 2913 (m), 2874 (m), 2827 (w), 1562 (m), 1491 (s), 1449 (m), 1235 (w), 1208 (vs), 1092 (vs), 1065 (s), 1028 (m), 918 (vs), 770 (s), 691 (m). UV–Vis (CH_3OH, nm): 288. TGA: temperature range, °C (% weight loss): 76–175 (33.1); 176–716 (41.5). DSC (°C): 109 (endo); 64 (endo). μ_{found} = 1.81 BM, g = 2.16 (300 and 77 K).

2.5. Structure determination

A suitable crystal of each compound, crystallized as described *vide supra*, was used for the diffraction studies. The diffraction intensity data have been obtained on a Nonius CAD4 diffractometer for **1**, on a STOE AED2 diffractometer for **2**, and on a Bruker Smart Apex diffractometer for **3**. The structure solution was achieved by direct methods as implemented in SHELXS-97 and the final refinement of the structures was carried using full least-squares methods on F^2 using SHELXL-97 [27]. The positions of hydrogen atoms attached to oxygen or nitrogen atoms were identified from the successive difference Fourier maps and were included in further calculations and refinement. The C–H hydrogen atoms were placed on calculated positions and refined using a riding model. The structure of **3** contains a void in the lattice, which has been filled with both a water dimer (50%) and a disordered MeOH (50%). Other details pertaining to data collection, structure solution and refinement are given in Table 1.

Table 1
Crystal data for compounds **1**–**3**.

	1	**2**	**3**
Identification code	rm61	mur57	rp275
Empirical formula	$C_{30}H_{62}Cu_1N_4O_{11}P_2$	$C_{28}H_{50}Cu_1N_2O_{10}P_2$	$C_{39}H_{46}CuN_2O_9P_2$
Formula weight	780.32	700.2	812.26
T (K)	293(2)	133(2)	100(2)
λ (Å)	0.71073	0.71073	0.71073
Crystal system	monoclinic	monoclinic	monoclinic
Space group	$P2_1/n$	$P2_1/n$	$C2/c$
a (Å)	12.389(3)	13.126(3)	13.8457(7)
b (Å)	10.263(2)	9.390(2)	15.5038(8)
c (Å)	16.314(2)	14.880(3)	17.8197(9)
β (°)	90.87(2)	112.15(3)	108.693(1)
V (Å^3)	2074.1(7)	1698.6(6)	3623.4(3)
Z	2	2	4
D_c (Mg/m^3)	1.249	1.369	1.489
Absolute coefficient (mm^{-1})	0.658	0.791	0.752
F(0 0 0)	834	742	1700
Crystal size (mm^3)	0.6 × 0.5 × 0.5	0.3 × 0.2 × 0.2	0.3 × 0.1 × 0.1
θ range (°)	2.05–24.98	2.62–24.89	4.19–25.02
Data/restraints/parameters	3641/20/246	2938/0/296	3199/5/243
Goodness-of-fit on F^2	1.118	1.027	1.078
R_1 [$I > 2\sigma(I)$]	0.0483	0.0311	0.0404
R_2 [$I > 2\sigma(I)$]	0.1345	0.0757	0.1152

3. Results and discussion

3.1. Synthesis and spectral characterization

The reaction between one equivalent of copper acetate and two equivalents of dtbp-H in the presence of two equivalents of pzet in methanol yields crystalline $[Cu(dtbp)_2(pzet)_2]\cdot H_2O$ (**1**) in good yield (Scheme 1). Similarly, the compounds, $[Cu(dtbp)_2(pyme)_2]$ (**2**) and $[Cu(dppi)_2(pyet)_2]$ (**3**) have been synthesized by the reaction of copper acetate with their corresponding phosphoryl ligand and co-ligand (**1**). Compounds **1**–**3** have been characterized by using elemental analysis, IR and UV–Vis spectroscopic studies, magnetic moment measurements and single crystal X-ray diffraction studies. The IR spectra of compounds **1–3** show broad peaks around 3400 cm^{-1} indicating the presence of free OH group from the alcohol side-arms of the co-ligands. The absence of any infrared absorption in the region of 2700–2500 cm^{-1} indicates the complete neutralization of dtbp-H/dppi-H in **1**–**3**. Strong bands observed at 1180, 1063 and 985 cm^{-1} for **1**, 1180, 1056 and 978 cm^{-1} for **2** and 1208, 1092 and 918 cm^{-1} for **3**, are due the POO and M–O–P vibrations [21].

The UV–Vis spectra of these complexes exhibit bands around 750 and 300 nm. These absorptions can be assigned to the d–d ($^2E_g \rightarrow {}^2T_{2g}$) transitions and combination of LMCT and π–π^* transitions, respectively. The ESR spectra of compounds **2** and **3** recorded as polycrystalline powder at 77 K as well as at room temperature show broad peaks with less resolved hyperfine structure [5]. The room temperature magnetic moments (μ_{eff} = 1.73 BM for **2** and 2.16 BM for **3**) are consistent with the monomeric Cu^{2+} complex. The high value of magnetic moment for **3** compared to **2** may indicate a partial contribution of the orbital angular momentum via spin–orbit coupling [5].

Although the composition of compounds **1**–**3** could be established from their analytical and spectroscopic data, the solid-state structure of all three compounds have been established by single crystal X-ray diffraction studies in order to obtain information on the molecular structure, including the role played by the –OH groups of the pyridinic co-ligands side arms. The details of the molecular structures are described below.

3.2. Molecular structure of *1*

Dark blue single crystals suitable for the diffraction studies were obtained by dissolving the compound $[Cu(dtbp)_2(pzet)_2]\cdot H_2O$ (**1**) in diethyl ether and storing the solution at −5 °C for 24 h. The compound crystallizes in the monoclinic $P2_1/n$ space group with half the molecule shown in Fig. 1 in the asymmetric part of the unit cell. The molecular structure reveals a monomeric structure for this compound. Two dtbp ligands coordinate to the central copper ion in a monodentate fashion through the de-protonated phosphate oxygen atom as in the case of the five coordinated copper–dtbp–phen complex $[Cu(phen)(dtbp)_2(OH_2)]$ [16]. However, the dtbp ligands adopt a *trans* configuration around the metal in the present case. The two pzet ligands are also coordinated to the central metal ion through the pyrazolyl nitrogen atom in a *trans* configuration, thus providing a square planar geometry around the metal. Quite interestingly, the hydroxyl group of the CH_2CH_2OH moiety in pzet ligands shows a positional disorder (which can best

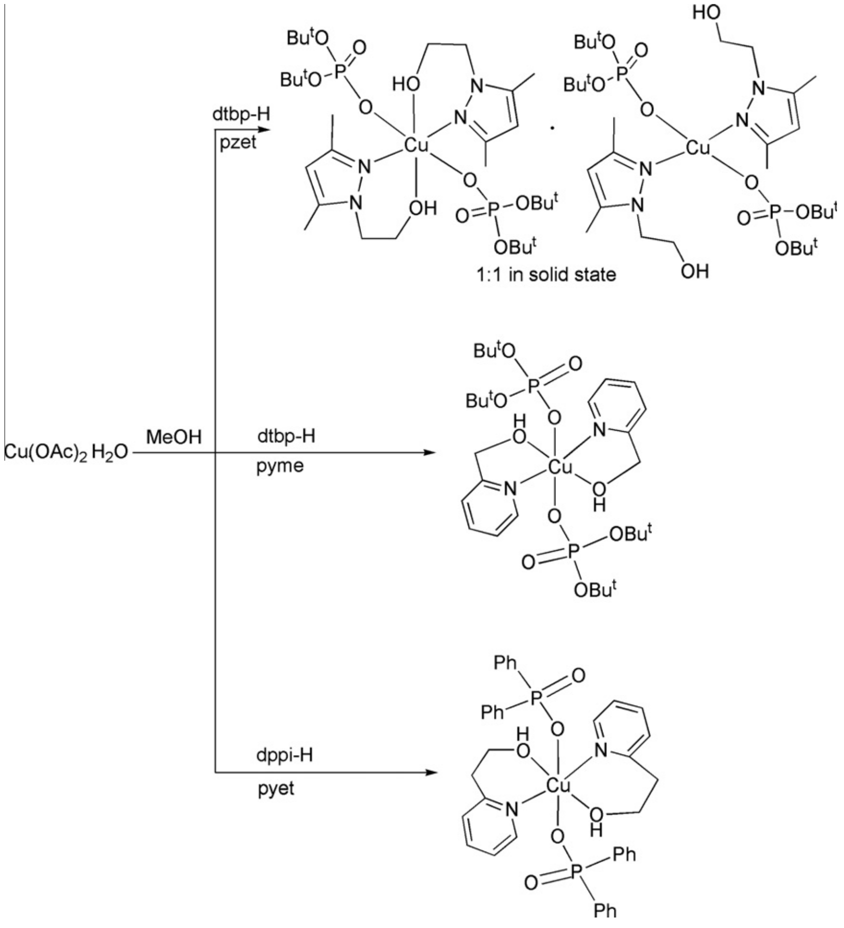

Scheme 1. Synthesis of $[Cu(dtbp)_2(pzet)_2]\cdot H_2O$ (**1**), $[Cu(dtbp)_2(pyme)_2]$ (**2**) and $[Cu(dppi)_2(pyet)_2]$ (**3**).

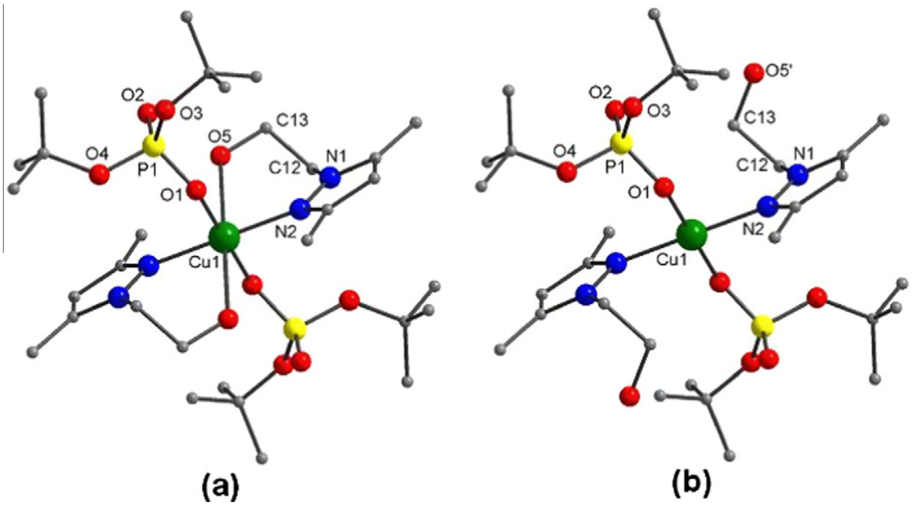

Fig. 1. Molecular structure of $[Cu(dtbp)_2(przet)_2]\cdot H_2O$ (**1**) showing (a) octahedral and (b) square planar geometry around copper atoms. Selected bond lengths (Å) and angles (°) Cu(1)–O(1) 1.939(2), Cu(1)–N(2) 2.025(2), Cu(1)–O(5) 2.485(6), P(1)–O(2) 1.460(3), P(1)–O(1) 1.504(2), P(1)–O(4) 1.572(2), P(1)–O(3) 1.593(3), O(1)–Cu(1)–O(1a) 180.0(2), N(2)–Cu(1)–N(2a) 180.0(2), O(1)–Cu(1)–N(2) 91.5(1), O(1a)–Cu(1)–N(2) 88.5(1), O(1)–Cu(1)–O(5) 94.0(2), O(1a)–Cu(1)–O(5) 86.0(2), N(2)–Cu(1)–O(5) 83.3(2), N(2a)–Cu(1)–O(5) 96.8(2), O(2)–P(1)–O(1) 116.5(2), O(2)–P(1)–O(4) 113.3(2), O(1)–P(1)–O(4) 105.6(1), O(2)–P(1)–O(3) 113.5(2), O(1)–P(1)–O(3) 106.9(2), O(4)–P(1)–O(3) 99.4(2), P(1)–O(1)–Cu(1) 133.8(2).

be termed as *rotational disorder about C–C axis*) with two positions for the hydroxyl group with equal occupancy (0.5:0.5) as schematically shown in Fig. 2. Since the CH_2CH_2OH chain is also conformationally flexible, one of the disordered –OH groups folds in such a manner that it is coordinated to the metal ion from the axial position, thus providing an octahedral geometry. The other half of the hydroxyl group points away from the metal center and is engaged in hydrogen bonding with the lattice water molecule present in the crystal (Fig. 1). For simplicity sake, these two positions are referred as "–OH in" and "–OH out".

The molecular structure of this complex is drawn twice in Fig. 1 (once with the atomic coordinates of "–OH in" and once with the atomic coordinates of "–OH out") to clearly show both 'octahedral' and 'square-planar' coordination geometries for the copper ion in the same complex.

The Cu–O(P) distance in **1** (1.939(2) Å) is slightly shorter than that observed for $[Cu(phen)(dtbp)_2(OH_2)]$ (1.974(3) and 1.975(4) Å) [16], but is longer than that observed in the case of copper polymer, $[Cu(dtbp)_2]_n$, 1.89(5) Å [15]. It should be noted that when dtbp ligand occupies the axial position in an octahedral complex, e.g., $[Cu(dtbp)_2(imz)_4]$ [28], this distance gets elongated to 2.475(1) Å. The observed Cu–N distance (2.025(2) Å) in **1** is comparable to the Cu–N(imidazole) distance in $[Cu(dtbp)_2(imz)_4]$ (2.006(2) and 2.045(2) Å). The Cu–O(axial) bond in the "–OH in" is elongated, as expected, and is in consistent with the Jahn–Teller elongation in d^9 copper systems (2.485(6) Å). The *cis* and *trans* L–Cu–L angles around the metal ion do not vary much from their ideal values 90 and 180°, respectively. The *cis* angles in **1** are in the range 83.3(2)–96.8(2)° while the observed *trans* angles are exactly 180° due to the center of symmetry lying at the metal center.

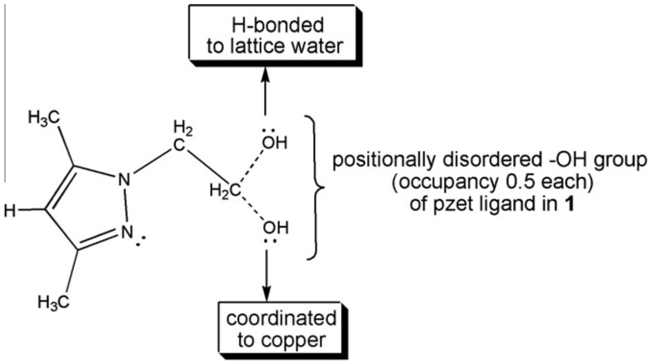

Fig. 2. Schematic representation showing the role of disordered –OH group in the molecular structure of **1**.

The crystal structure of **1** shows interesting H-bonding interactions assisted by four unique hydrogen bonds. For example, the $–CH_2CH_2OH$ group (O(5)) of the pzet ligand when present in "–OH in" form, forms an intramolecular hydrogen bond to the P═O group (O(2)) of the coordinated dtbp ligand (2.663 Å). When the same group is present in the "–OH out form", it is engaged in hydrogen bonding with the lattice water (O(5′)···O(6) 2.827 Å). In addition to this there are two more hydrogen bonds involving the lattice water and the phosphoryl oxygen atoms (O(2)···O(6) 2.894 and 2.778 Å). Thus the presence of a lattice water molecule (O(6)) in the crystal of **1** along with the conformationally flexible $–CH_2CH_2OH$ group is responsible for the 1D supramolecular assembly formation shown in Fig. 3.

3.3. Molecular structure of **2**

Compound **2** has been crystallized from acetonitrile/methanol mixture. The centrosymmetric compound **2** crystallizes in the monoclinic $P2_1/n$ space group with half of the molecule in the asymmetric part of the unit cell. The molecular structure of **2** (Fig. 4) can best be described as the "–OH in" form of **1**. Thus, the pyme ligands in **2** form five-membered chelate rings. The absence of "–OH out" form in **2** could be ascribed to the shorter $–CH_2OH$ side chain on the pyridine. The coordination geometry around the central copper(II) ion **2** hence is axially elongated octahedron. The metal is surrounded by two phosphate oxygen atoms (Cu1–O1, 2.010(2) Å), two pyridine nitrogen atoms (Cu1–N1, 1.988(2) Å), and two $–CH_2OH$ groups (Cu1–O5, 2.357(2) Å). Each of the ligand types binds the metal ion in a *trans* configuration as shown in Fig. 4. The bond distances are in agreement with the values described above for compound **1**. The *cis* angles around the metal ion do not deviate appreciably from its ideal value 90° (78.16(6)–101.84(6)°), while the observed *trans* angles are 180° due to molecule's center of symmetry at the metal center.

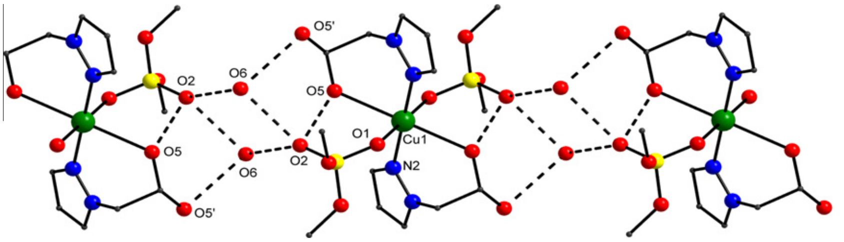

Fig. 3. Formation of 1D supramolecular assembly in **1** aided by intra- and intermolecular H-bonds. Hydrogen atoms and the methyl groups on pyrazole and *tert*-butyl substituents are omitted for clarity. O5 and O5′ represent the two positions for the ethanol oxygen.

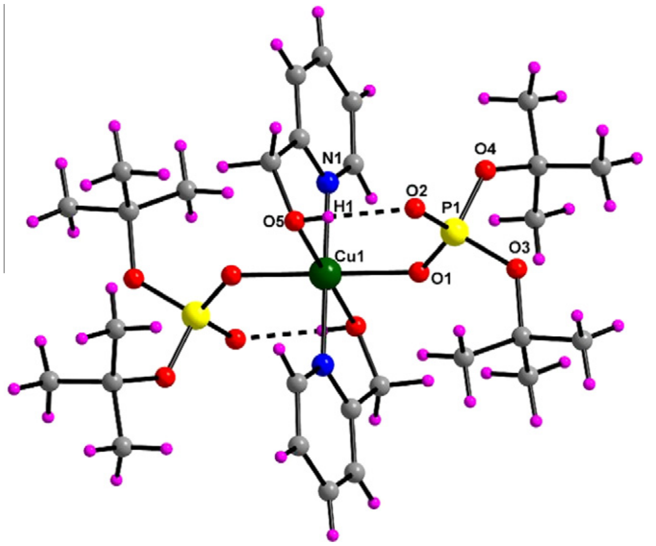

Fig. 4. Molecular structure of [Cu(dtbp)$_2$(pyme)$_2$] (**2**). Selected bond lengths (Å) and angles (°): Cu(1)–O(1) 2.010(2), Cu(1)–O(5) 2.357(2), Cu(1)–N(1) 1.988(2), P(1)–O(1) 1.511(2), P(1)–O(2) 1.495(2), P(1)–O(3) 1.588(2), P(1)–O(4) 1.586(2); O(1)#1–Cu(1)–O(1) 180.0, O(5)#1–Cu(1)–O(5) 180.0, N(1)#1–Cu(1)–N(1) 180.0, O(1)–Cu(1)–O(5) 93.84(6), O(1)–Cu(1)–O(5)#1 86.16(6), N(1)–Cu(1)–O(1) 91.30(7), N(1)–Cu(1)–O(1)#1 88.70(7), N(1)–Cu(1)–O(5) 78.16(6), N(1)–Cu(1)–O(5)#1 101.84(6), O(2)–P(1)–O(1) 115.16(9), O(2)–P(1)–O(4) 105.92(8), O(1)–P(1)–O(4) 111.93(8), O(2)–P(1)–O(3) 112.03(9), O(1)–P(1)–O(3) 109.85(8), O(4)–P(1)–O(3) 101.00(8). Symmetry transformations used to generate equivalent atoms: (#1) $2 - x, -y, 2 - z$.

The intramolecular hydrogen bond (O5–H1···O2, 2.600(3) Å) creates a six-membered metallocycle Cu–O–H–O–P–O, which further stabilizes the molecular structure. The crystals of **2** do not possess lattice water molecule as in **1**. However, the pyridine C–H bonds act as the source of intermolecular hydrogen bonding with the adjacent molecule's phosphate oxygen atoms to form a 1D chain like structure as shown in Fig. 5 (C(12)–H(12)···O(4) 3.368(3); C(13)–H(13)···O(2) 3.301(3) Å).

3.4. Molecular structure of 3

The singe crystals of **3** obtained from acetonitrile/methanol solution, crystallize in monoclinic *C*2/*c* space group with half of the molecule occupying the asymmetric part of the unit cell. The molecular structure of **3** is very similar to **2** (Fig. 6) although the co-ligand used in **3** is pyet and not pyme. Similarly, the dtbp ligand in **2** has been replaced by dppi in **3**. Hence the coordination geometry around the central copper(II) ion **3** is Jahn–Teller elongated octahedron. The metal is surrounded by two phosphate oxygen atoms (Cu1–O2, 2.025(2) Å), two pyridine nitrogen atoms (Cu1–N1 2.017(2) Å) and two oxygen atoms from two pyet side chains (Cu1–O1, 2.385(2) Å). As in the case of **1** and **2** described above, each of the ligand types in **3** bind the metal ion in a *trans* configuration; the bond distances mentioned are also in agreement with the corresponding values found in **1** and **2**, and similar complexes. The *cis* angles around the metal ion do not deviate appreciably from its ideal value 90° (87.0(1)–93.0(1)°) while the observed *trans* angles are 180° owing to molecule's center of symmetry lying on the metal center.

3.5. Comparison of structures of 1–3

The molecular structures of **1**–**3** are essentially similar in the sense that they all contain Cu(II) ion which is surrounded by either two dialkyl phosphate or diaryl phosphinate ligands existing in a monodentate terminal fashion and two chelating pyrazole or pyridine co-ligands bearing a alcohol side chain (either –CH$_2$OH or –CH$_2$CH$_2$OH). In the case of **1**, however, the high flexibility of the –CH$_2$CH$_2$OH chain leads to both monodentate and chelating forms of the pyrazole ethanol. This is probably aided by both crystal packing effects as well as the length of the chain itself. The conformation of the six- or five-membered chelate rings in the structure of **1**–**3** is pictorially depicted in Fig. 7, which reveals the highly non-planar nature of the rings. Because of the presence of –OH groups, uncoordinated phosphoryl P═O groups, and also lattice water (in case of **1**), a number of intra- and intermolecular hydrogen bonds are formed in the crystal lattice.

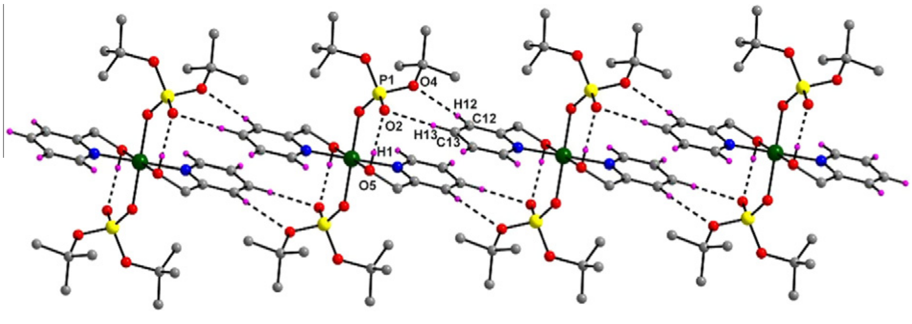

Fig. 5. Hydrogen bonding pattern in [Cu(dtbp)$_2$(pyme)$_2$] (**2**) (hydrogen atoms on the methyl groups are removed for the clarity).

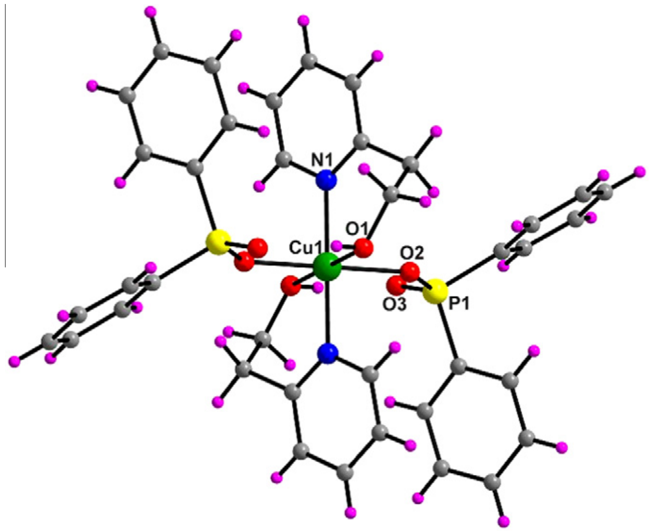

Fig. 6. Molecular structure of [Cu(dppi)$_2$(pyet)$_2$] (**3**). Selected bond lengths (Å) and angles (°): Cu(1)–O(1) 2.385(2), Cu(1)–O(2) 2.025(2), Cu(1)– N(1) 2.017(2), P(1)–O(3) 1.508(2), P(1)–O(2) 1.517(2); O(3)–P(1)–O(2) 115.9(1), O(1)–Cu(1)–O(1)#1 180.0(1), O(2)–Cu(1)–O(2)#1 180.0(1), N(1)–Cu(1)–N(1)#1 180.0, O(2)–Cu(1)–O(1) 90.9(1), O(2)–Cu(1)–O(1)#1 89.1(1), N(1)–Cu(1)–O(1) 87.0(1), N(1)#1–Cu(1)–O(1) 93.0(1), N(1)–Cu(1)–O(2) 88.7(1), N(1)–Cu(1)–O(2)#1 91.4(1). Symmetry transformations used to generate equivalent atoms: (#1) $2 - x, -y, 1 - z$, (#2) $1 - x, y, 1/2 - z$.

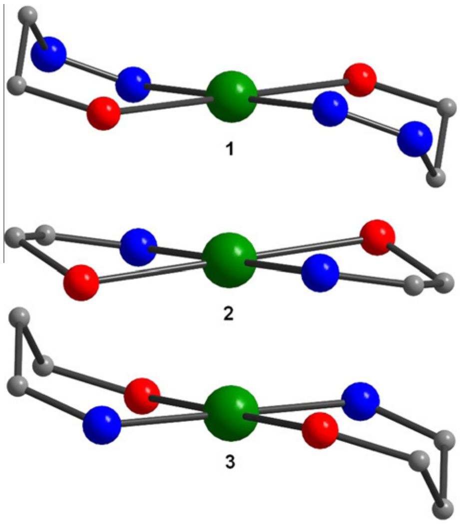

Fig. 7. Comparison of the conformation of the chelate rings in the structures of **1**–**3**.

4. Conclusion

We have presented in this contribution the synthesis and structural characterization of a series of Cu(II) complexes bearing monoprotic phosphorus acids (dialkyl phosphate and diaryl phosphinate). The use of a co-ligand in the form of 2-pyrazole ethanol and 2-pyridine methanol/ethanol in these reactions serves to block the oligomerization through chelation, and hence only monomeric compounds have been isolated (in contrast to isolation of polymeric and oligomeric complexes isolated earlier with phosphorus based acids). The conformationally very flexible ethanol side chain of the co-ligand in **1** led to the realization of both square planar and octahedral coordination environments for copper in this complex. Thus the results presented here complement our earlier studies on copper dtbp complexes with strictly monodentate [12,28], strictly bidentate chelating [13,16] and bidentate bridging ligands [21,22], as well as copper monoaryl phosphate complexes [11].

Acknowledgements

This work was supported by DST, New Delhi. R.P. thanks CSIR, Delhi for a senior research fellowship. The authors thank the SAIF, IIT-Bombay for spectral data and National Single Crystal Diffraction Facility for the X-ray data for **1**.

Appendix A. Supplementary material

CCDC 791906–791908 for compounds **1**–**3** contain the supplementary crystallographic data for this paper. These data can be obtained free of charge from The Cambridge Crystallographic Data Centre via www.ccdc.cam.ac.uk/data_request/cif. Supplementary data associated with this article can be found, in the online version, at doi:10.1016/j.ica.2011.03.063.

References

[1] A. Mohindru, J.M. Fisher, M. Rabinnovitz, Nature 303 (1983) 64.
[2] J.D. Ranford, P.J. Sadler, D.A. Tocher, J. Chem. Soc., Dalton Trans. (1993) 3393.
[3] F.T. Greenaway, A. Pezeshk, A.W. Cordes, M.C. Noble, J.R.J. Sorenson, Inorg. Chim. Acta 93 (1984) 67.
[4] J. Sokolík, M. Blahová, G. Cukanová, M. Kohutová, E. Mišíková, D. Mlynarčík, Čes. Slov. Farm. 47 (1998) 186.
[5] Z. Púčeková-Repická, J. Moncol, D. Valigura, T. Lis, M. Korabik, M. Melník, J. Mroziński, M. Mazúr, J. Coord. Chem. 60 (2007) 2449.
[6] J.R.J. Sorenson, J. Med. Chem. 19 (1976) 135.
[7] J.R.J. Sorenson, Prog. Med. Chem. 15 (1978) 211.
[8] R. Murugavel, A. Choudhury, M.G. Walawalkar, R. Pothiraja, C.N.R. Rao, Chem. Rev. 108 (2008) 3549.
[9] R. Murugavel, N. Gogoi, J. Organomet. Chem. 695 (2010) 916.
[10] J. Pinkas, D. Chakraborty, Y. Yang, R. Murugavel, M. Noltemeyer, H.W. Roesky, Organometallics 18 (1999) 523.
[11] R. Murugavel, S. Kuppuswamy, A.N. Maity, M.P. Singh, Inorg. Chem. 48 (2009) 183.
[12] R. Murugavel, M. Sathiyendiran, R. Pothiraja, M.G. Walawalkar, T. Mallah, E. Riviere, Inorg. Chem. 43 (2004) 945.
[13] R. Murugavel, R. Pothiraja, N. Gogoi, R. Clerac, L. Lecren, R.J. Butcher, M. Nethaji, Dalton Trans. (2007) 2405.
[14] V. Chandrasekhar, R. Azhakar, T. Senapati, P. Thilagar, S. Ghosh, S. Verma, R. Boomishankar, A. Steiner, P. Kögerler, Dalton Trans. (2008) 1150.
[15] M. Sathiyendiran, R. Murugavel, Inorg. Chem. 41 (2002) 6404.
[16] R. Murugavel, M. Sathiyendiran, R. Pothiraja, R.J. Butcher, Chem. Commun. (2003) 2546.
[17] M.G. Walawalkar, H.W. Roesky, R. Murugavel, Acc. Chem. Res. 32 (1999) 117.
[18] R. Murugavel, S. Shanmugan, Chem. Commun. (2007) 1257.
[19] R. Murugavel, S. Kuppuswamy, N. Gogoi, R. Boomishankar, A. Steiner, Chem. Eur. J. 16 (2010) 994.
[20] R. Murugavel, S. Kuppuswamy, R. Boomishankar, A. Steiner, Angew. Chem., Int. Ed. 45 (2006) 5536.
[21] R. Pothiraja, M. Sathiyendiran, R.J. Butcher, R. Murugavel, Inorg. Chem. 44 (2005) 6314.
[22] R. Pothiraja, M. Sathiyendiran, R.J. Butcher, R. Murugavel, Inorg. Chem. 43 (2004) 7585.
[23] Y. Murakami, M. Tokunaga, Bull. Chem. Soc. Jpn. 37 (1964) 1562.
[24] N. Lah, I. Leban, R. Clérac, Eur. J. Inorg. Chem. (2006) 4888.
[25] D.D. Perrin, W.L.F. Armarego, Purification of Laboratory Chemicals, third ed., Pergamon Press, Oxford, 1988.
[26] A. Zwierzak, M. Kluba, Tetrahedron 27 (1971) 3163.
[27] G.M. Sheldrick, Acta Crystallogr., Sect. A 64 (2008) 112.
[28] R. Murugavel, M. Sathiyendiran, Chem. Lett. (2001) 84.